Acta Geotechnica (2018) 13:1313–1327
https://doi.org/10.1007/s11440-018-0716-8

RESEARCH PAPER

A rheological model to simulate the shear creep behavior of rockfills considering the influence of stress states

Ming Xu[1] · Dehai Jin[1] · Erxiang Song[1] · Dawei Shen[1]

Received: 17 September 2017 / Accepted: 10 September 2018 / Published online: 24 October 2018

Abstract

Rockfills have been extensively used in the construction of high-fill embankments and dams, which exhibit complex time-dependent behavior. This paper presents a rheological model to simulate the shear creep behavior of rockfills based on the classic Burgers model, in which a nonlinear elasto-damage unit, a modified Newton unit, and a modified Kelvin unit are connected in series. By analyzing the results of large-scale triaxial creep tests on different rockfills, the influence of stress states (i.e., the deviator stress level and confining pressure) on the shear creep behavior of rockfills is revealed. A method to modify the key model parameters is proposed to consider such influence and is incorporated into the proposed model. Furthermore, the accelerated creep behavior of rockfills is reproduced by a nonlinear elasto-damage unit. Despite its simplicity, the model can simulate the essential aspects of the shear creep behavior of rockfills, and reasonable consistency is found between the simulation results and the large-scale triaxial creep test results.

Keywords Accelerated creep · Confining pressure · Damage mechanism · Deviator stress level · Rockfills

List of symbols

a	Parameter of the modified Kelvin unit
C	$C = C_{\text{ref}}\left(\frac{\sigma_3}{p_a}\right)^m$
C_{ref}	Parameter of the nonlinear elasto-damage unit
D	Deviator stress level, $D = (\sigma_1 - \sigma_3)/(\sigma_1 - \sigma_3)_f$
D_{thr}	Critical threshold of the deviator stress level
E	Young's modulus
E_t	Initial tangent modulus
G^K	Shear modulus of the Kelvin unit
K_1	Parameter of the nonlinear elasto-damage unit
K_2	Parameter of the modified Newton unit
K_3	Parameter of the modified Kelvin unit
K_4	Parameter of the modified Kelvin unit
m	Parameter of the nonlinear elasto-damage unit
n_1	Parameter of the nonlinear elasto-damage unit
n_2	Parameter of the modified Newton unit
n_3	Parameter of the modified Kelvin unit
n_4	Parameter of the modified Kelvin unit
p_a	Atmospheric pressure
q_i	Deviator stress, $q_i = \sigma_i - \sigma_{kk}/3$
R_f	$R_f = (\sigma_1 - \sigma_3)_f \Big/ (\sigma_1 - \sigma_3)_{\text{ult}}$
S	Overall section area of the damage unit
S_ω	Total area of the microcracks and cavities with different shapes
t	Creep time
t_{ref}	Referenced time t_{ref} is set to be one hour in this paper
t_{ult}	Ultimate time, $t_{\text{ult}} = 1/[C(1+V)D^V]$
V	Parameter of the nonlinear elasto-damage unit
γ	$\gamma = 1/(1+V)$
ε_i	Total strain, subscript $i = 1, 2, 3$
ε_1^0	Axial transient strain
ε_i^B	Strain of the Burgers unit

✉ Erxiang Song
songex@mail.tsinghua.edu.cn

Ming Xu
mingxu@mail.tsinghua.edu.cn

Dehai Jin
jdh14@mails.tsinghua.edu.cn

Dawei Shen
sdw13@mails.tsinghua.edu.cn

[1] Department of Civil Engineering, Tsinghua University, Beijing 100084, China

$\dot{\varepsilon}_i^B(0^+)$	Strain rate of Burgers model when $t = 0^+$
$\dot{\varepsilon}_i^B(\infty)$	Strain rate of Burgers model when $t = \infty$
ε_i^D	Strain of the nonlinear elasto-damage unit
ε_i^E	Elastic strain of the linear spring unit
ε_i^K	Strain of the Kelvin unit
$\varepsilon_i^{K,M}$	Strain of the modified Kelvin unit
ε_i^N	Viscous strain of the Newton unit
$\varepsilon_i^{N,M}$	Strain of the modified Newton dashpot unit
$\varepsilon_i^{\text{ref}}$	Referenced strain in the accelerated creep stage
$\Delta\varepsilon_i^D$	Strain of the unit in the damage deformation stage
η^K	Viscosity coefficient of the Kelvin unit
η^N	Viscosity coefficient of the Newton unit
υ	Poisson's ratio
$(\sigma_1 - \sigma_3)_f$	Peak deviator stress
$(\sigma_1 - \sigma_3)_{\text{ult}}$	Asymptotic value of $(\sigma_1 - \sigma_3)$ when the stress–strain curve approaches infinite strain
σ_i	Principal stress
σ_{kk}	$\sigma_{kk} = \sigma_1 + \sigma_2 + \sigma_3$
ω	Damage variable, $\omega = S_\omega / S$

1 Introduction

In recent years, more and more high-fill embankments and dams in mountainous areas have been planned and constructed [13–15, 22, 29]. Rockfills have been extensively used for the construction of these high-fill embankments and dams. In general, rockfills exhibit many complex mechanical properties, i.e., nonlinear stress–strain behavior, stress-level-dependent behavior, and other properties, which have been investigated extensively in past studies [2, 5, 31, 32]. Furthermore, these embankments and dams have been observed to deform with time [8, 19, 28], which may cause serviceability problems and even failures. To ensure the long-term safety of such high-fill structures, a study on the creep characteristics of rockfills is desirable. Finite element analysis is usually adopted for realistic deformation prediction of these engineering problems, which requires an accurate constitutive model that considers the time-dependent properties of rockfills [4, 7, 24–26, 30, 35]. Discrete element method has also been used in recent years to study the micro-mechanism of the creep behavior of rockfills [21, 33, 38].

Laboratory tests have been conducted to study the time-dependent behavior of rockfills [3, 6, 10, 11]. Anhdan et al. [3] investigated the viscous behavior of gravelly soils subjected to drained triaxial compression and found that particle crushing produces more creep deformation at higher stresses. Enomoto et al. [10] conducted a large-scale triaxial compression test on an air-dried well-graded Shinanogawa riverbed gravel, which consists of round gravels and relatively angular sand particles. Creep deformation was revealed to increase with increasing sustained deviator stress levels, which is defined as $D = (\sigma_1 - \sigma_3)/(\sigma_1 - \sigma_3)_f$, where $(\sigma_1 - \sigma_3)_f$ is the peak deviator stress. Chen and Zhang [6] developed a new large triaxial creep apparatus, and tertiary rheological behavior was observed when redstone granular soils were subjected to a high deviator stress level ($D = 0.8$). Enomoto et al. [11] evaluated the creep failure behavior of a natural gravelly soil by performing drained sustained tests at the prescribed stress states after monotonic loading at different loading rates. These test results indicate that the creep behaviors of rockfills are influenced by the stress state (deviator stress level and confining pressure) and loading rate.

Based on experimental observations, typical strain–time curves for rockfills are presented in Fig. 1, where the creep deformation can be generally categorized into three stages: (1) the attenuated creep stage with a decreasing strain rate (segment AB); (2) the steady creep stage with a constant strain rate (segment BC); and (3) the accelerated creep stage with an increasing strain rate (segment CE).

Developing appropriate constitutive models to simulate the creep behavior of rockfills based on physical tests is important. In general, the creep models of geomaterials can be classified into three categories: empirical models, rheological models, and general stress–strain–time models [20]. Zhou et al. [37] proposed an empirical model based on experimental results, in which the creep strain of rockfills is expressed as a function of elapsed time, confining pressure, and deviator stress level. Then, a numerical simulation procedure was proposed such that this empirical model can be used with the general finite element method

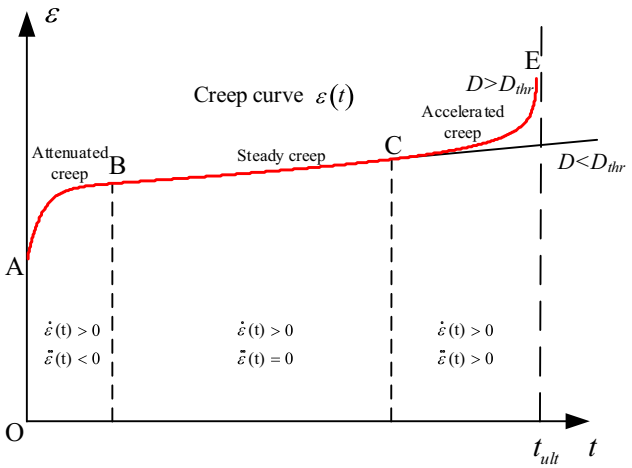

Fig. 1 Schematic view of the strain–time curve for rockfills

to predict the long-term deformation of high rockfill dams. The differential approach of the rheological model (i.e., Maxwell model, Kelvin model, Burgers model, etc.) is composed of elastic springs, plastic sliders, and viscous dashpots. These types of models have been extensively used in geotechnical engineering due to their simple creep constitutive equations and the clear physical meanings of the model parameters. However, most rheological models have been developed for rock and fine-grained soils (e.g., sand, clay, etc.). Few rheological models can generate a reasonable simulation of the shear creep behavior of rockfills, in which particle breakage plays an important role and is influenced by the stress states. Furthermore, the accelerated creep behavior of rockfills has only been revealed in the laboratory in recent years [6], which also need to be considered in a constitutive model.

To describe the shear creep behavior of rockfills under different stress states, a rheological model is proposed in this paper. The influence of deviator stress levels and confining pressures on the shear creep characteristics of rockfills is investigated by analyzing the results of large-scale triaxial creep tests on different rockfills. A method to modify the key model parameters so that such an influence can be considered is proposed and incorporated into the proposed model. Furthermore, the accelerated creep strain of rockfills is reproduced by introducing a nonlinear elasto-damage unit. A simple calibration procedure is proposed to determine model parameters from experimental results. Compared with the results of large-scale triaxial creep tests on three types of rockfills, this simple model proves that it can predict the shear creep behavior of rockfills with fairly high accuracy.

2 Framework of this paper

The proposed model for rockfills is modified from the classical Burgers model and is schematically characterized by three modified components connected in series, including a nonlinear elasto-damage unit, a modified Newton unit and a modified Kelvin unit, as seen in Fig. 2. The total strain ε_i at time t is the sum of the strains of these three components:

$$\varepsilon_i = \varepsilon_i^D + \varepsilon_i^{N,M} + \varepsilon_i^{K,M} \tag{1}$$

where ε_i^D is the strain of the nonlinear elasto-damage unit, $\varepsilon_i^{N,M}$ is the strain of the modified Newton dashpot unit, $\varepsilon_i^{K,M}$ is the strain of the modified Kelvin unit, and subscript $i = 1, 2, 3$. It should be noted that the superscripts D, N, and K denote the damage, Newton, and Kelvin units, respectively. The superscript M denotes that the unit has been modified from the original unit.

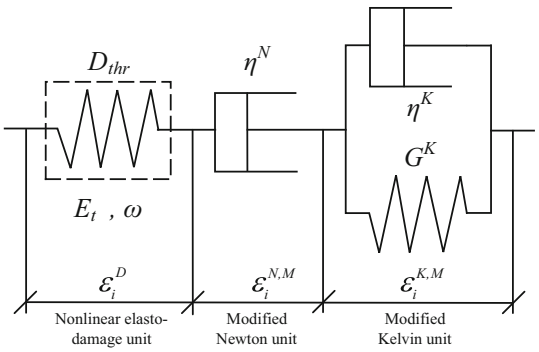

Fig. 2 Schematic view of the shear creep constitutive model for rockfills

This paper is structured as follows. In Sect. 3, a calibration method is proposed to determine the parameters of the classical Burgers model. In Sect. 4, the classical Burgers model is modified to consider the influence of the confining pressure and deviator stress level. In Sect. 5, based on the Kachanov damage mechanism, a nonlinear elasto-damage unit is proposed to capture the accelerated creep behavior of rockfills. In Sect. 6, a brief summary of the shear creep model is presented. Finally, in Sect. 7, the results of three sets of large-scale triaxial creep tests are used to validate the effectiveness of the proposed model.

3 Calibration method for the classical Burgers model

The classical Burgers model consists of a linear spring unit (Young's modulus E and Poisson's ratio υ), a Newton unit (viscosity coefficient η^N), and a Kelvin unit (shear modulus G^K and viscosity coefficient η^K), as illustrated in Fig. 3. Thus, the classical Burgers model is a five-parameter model (G^K, η^K, η^N, E, and υ). The Poisson ratio υ has a minor influence on the simulation results and is usually set as 0.3 for rockfills.

The total strain ε_i^B at time t is expressed in Eq. (2):

$$\varepsilon_i^B = \varepsilon_i^E + \varepsilon_i^N + \varepsilon_i^K \tag{2}$$

where ε_i^B is the strain of the Burgers unit, ε_i^E is the elastic strain of the linear spring unit, ε_i^N is the viscous strain of the Newton unit, and ε_i^K is strain of the Kelvin unit. The superscript B denotes the Burgers unit. The constitutive equations of these three units were presented by Findley et al. [12] as:

$$\varepsilon_i^E = \frac{(1+\upsilon)\sigma_i - \upsilon\sigma_{kk}}{E} \tag{3}$$

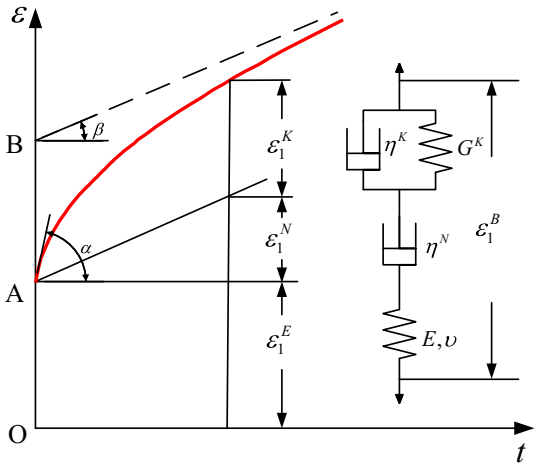

Fig. 3 Schematic view of the classical Burgers model

$$\varepsilon_i^N = \frac{q_i}{2\eta^N} t \tag{4}$$

$$\varepsilon_i^K = \frac{q_i}{2G^K}\left[1 - \exp\left(-\frac{G^K}{\eta^K} t\right)\right] \tag{5}$$

$$\varepsilon_{i,t\to\infty}^K = \frac{q_i}{2G^K} \tag{6}$$

where σ_i is the principal stress; $\sigma_{kk} = \sigma_1 + \sigma_2 + \sigma_3$; q_i is the deviator stress, $q_i = \sigma_i - \sigma_{kk}/3$. As shown in Fig. 3, the segment OA represents the instantaneous elastic strain, which can be calculated from Eq. (3). By combining Eqs. (2)–(5), the strain of the classical Burgers model at time t is obtained as:

$$\varepsilon_i^B = \frac{(1+\upsilon)\sigma_i - \upsilon\sigma_{kk}}{E} + \frac{q_i}{2\eta^N} t + \frac{q_i}{2G^K}\left[1 - \exp\left(-\frac{G^K}{\eta^K} t\right)\right] \tag{7}$$

Then, the creep rate can be expressed as:

$$\dot{\varepsilon}_i^B = \frac{q_i}{2\eta^N} + \frac{q_i}{2\eta^K}\exp\left(-\frac{G^K}{\eta^K} t\right) \tag{8}$$

The creep rates at $t = 0^+$ and $t = \infty$ are presented in Eqs. (9) and (10), respectively:

$$\dot{\varepsilon}_i^B(0^+) = \frac{q_i}{2\eta^N} + \frac{q_i}{2\eta^K} = \tan\alpha \tag{9}$$

$$\dot{\varepsilon}_i^B(\infty) = \frac{q_i}{2\eta^N} = \tan\beta \tag{10}$$

A calibration method is proposed here to determine the four parameters (G^K, η^K, η^N, and E) from the results of the creep test on redstone granular soil ($\sigma_3 = 100$ kPa and $D = 0.6$) performed by Chen and Zhang [6], as shown in Fig. 4.

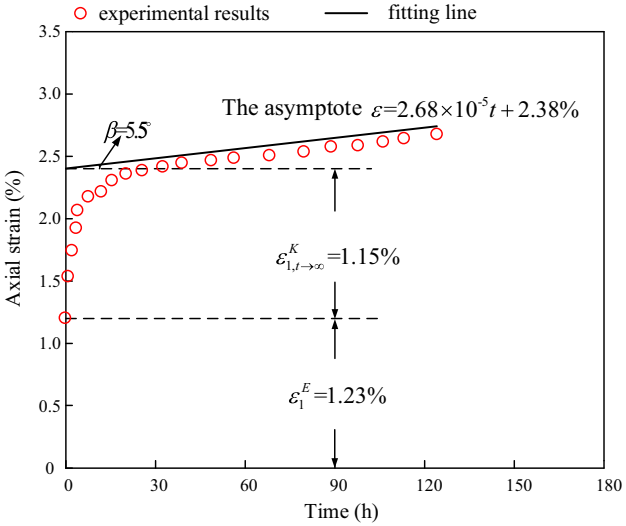

Fig. 4 Procedure to determine the parameters of the classical Burgers model for redstone granular soil ($D = 0.6$ and $\sigma_3 = 100$ kPa, [6])

3.1 The Young's modulus *E*

In Fig. 4, by substituting the instantaneous strain ($\varepsilon_1^E = 1.23\%$, i.e., OA in Fig. 3) and the stress states ($\sigma_1 = 684$ kPa, $\sigma_3 = 100$ kPa, $D = 0.6$) into Eq. (3), the Young's modulus E can be obtained.

3.2 The Newton viscosity coefficient η^N

An asymptote to the creep test curve is drawn in Fig. 4, where β is the incline angle of the asymptote. Thus, by substituting the value of β (5.5°) and $q_1 = 2(\sigma_1 - \sigma_3)/3 = 390$ kPa into Eq. (10), the value of η^N can be calculated.

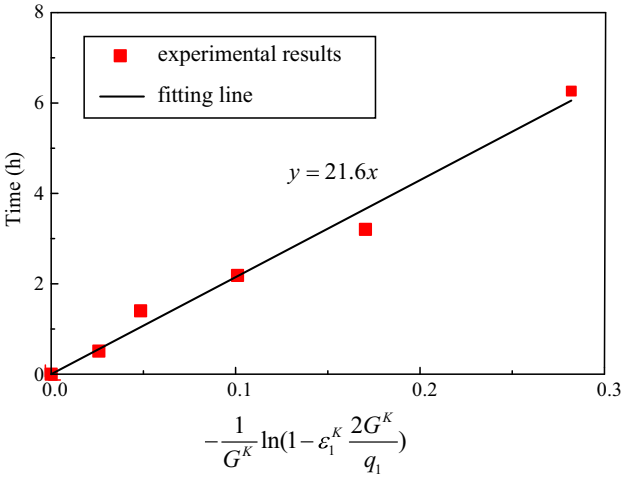

Fig. 5 $t - \left[-\frac{1}{G^K}\ln\left(1 - \varepsilon_1^K \frac{2G^K}{q_1}\right)\right]$ curve and the fitting results for redstone granular soil ($D = 0.6$ and $\sigma_3 = 100$ kPa, [6])

Table 1 Parameters of the classical Burgers model for the creep test of the redstone granular soil ($D = 0.6$ and $\sigma_3 = 100$ kPa, [6])

E (MPa)	η^N (MPa h)	G^K (MPa)	η^K (MPa h)
51.9	6332	17.3	21.6

3.3 The Kelvin shear modulus G^K

By substituting the stable Kelvin strain ($\varepsilon^K_{1,t\to\infty} = 1.15\%$, i.e., AB in Fig. 3) and the corresponding deviator stress value ($q_1 = 390$ kPa) into Eq. (6), the value of G^K can be obtained.

3.4 The Kelvin viscosity coefficient η^K

As shown in Eq. (9), the η^K value can be back-calculated when the initial tangent angle α is determined. However, it is difficult to determine α directly from the test data, as shown in Fig. 4. Thus, Eq. (5) is rewritten as:

$$t = \eta^K \left[-\frac{1}{G^K} \ln\left(1 - \varepsilon_1^K \frac{2G^K}{q_1}\right) \right] \tag{11}$$

The axial Kelvin strain (ε_1^K) at time t can be separated from the total axial strain according to Eqs. (2)–(4). Therefore, t is plotted against $-\frac{1}{G^K}\ln\left(1 - \varepsilon_1^K \frac{2G^K}{q_1}\right)$ in Fig. 5, and the slope of the fitting line equals the value of η^K.

Using the above calibration method, the four parameters are obtained and summarized in Table 1.

4 Modified Burgers model for rockfills without considering the accelerated creep behavior

The results of large-scale triaxial creep tests on three different types of rockfills are analyzed, and the parameters of the classic Burgers model are determined for each individual test. The influence of the deviator stress level and confining pressure on these parameters is investigated, based on which a modified Burgers model is proposed. Only the deformations of the first two creep stages (i.e., segments AB and BC in Fig. 1) are investigated here, whereas the third creep stage (i.e., the accelerated creep stage) will be further discussed in Sect. 5.

Information regarding these three sets of tests [6, 27, 36] is summarized in Table 2. By using the calibration method proposed in Sect. 3, the parameters (η^N, η^K, and G^K) of these rockfills are determined from each individual test (i.e., with different deviator stress levels and confining pressures). As shown in Tables 3, 4, and 5, these parameters vary with the deviator stress level and confining pressure. Thus, this section aims to find the mathematical relation between these parameters and the stress states. Furthermore, the parameter E is also modified to describe the nonlinear stress–strain behavior of rockfills.

Table 3 η^N values under different confining pressures and deviator stress levels for the three rockfills [6, 27, 36]

η^N (MPa h)	σ_3 (MPa)	$D = 0.2$	$D = 0.4$	$D = 0.6$	$D = 0.8$
Rockfills from Shangzhai	0.5	25,303	17,183	15,839	14,675
	1	27,081	30,723	27,588	27,604
	2	63,477	53,011	59,463	43,973
	3	90,920	106,834	71,346	125,141
Redstone granular soil	0.05	–	6066	6104	6431
	0.1		7630	6332	7533
	0.2		7890	6538	8072
	σ_3 (MPa)	$D = 0.25$	$D = 0.5$	$D = 0.75$	–
Rockfills from Dalian	0.4	129,764	105,817	112,194	–
	0.8	141,999	122,202	137,200	
	1.2	169,223	166,007	178,970	

Table 2 Initial properties of the specimens and testing programs of the triaxial creep tests

References	Material	Dry density (kN/m^3)	Height (mm)	Diameter (mm)	σ_3 (MPa)	D
Chen and Zhang [6]	Redstone granular soil	18.8	600	300	0.20	0.4
					0.10	0.6
					0.05	0.8
Wang [27]	Limestone rockfills from Dalian	19.8	600	300	1.2	0.25
					0.8	0.50
					0.4	0.75
Zhang [36]	Quarried sandstone rockfills from Shangzhai	20.6	700	300	3	0.2
					2	0.4
					1	0.6
					0.5	0.8

Table 4 η^K values under different confining pressures and deviator stress levels for the three rockfills [6, 27, 36]

η^K (MPa h)	σ_3 (MPa)	$D = 0.2$	$D = 0.4$	$D = 0.6$	$D = 0.8$
Rockfills from Shangzhai	0.5	37.4	43.7	39.6	45.3
	1	55.8	43.0	47.8	42.2
	2	65.5	58.7	67.7	65.3
	3	86.7	70.8	70.4	68.5
Redstone granular soil	0.05	–	22.0	17.3	22.2
	0.1		23.4	21.6	23.4
	0.2		25.3	21.5	26.7
	σ_3 (MPa)	$D = 0.25$	$D = 0.5$	$D = 0.75$	–
Rockfills from Dalian	0.4	207.0	253.6	255.6	–
	0.8	310.5	316.6	304.4	
	1.2	439.9	356.2	419.9	

Table 5 G^K values under different confining pressures and deviator stress levels for the three rockfills [6, 27, 36]

G^K (MPa)	σ_3 (MPa)	$D = 0.2$	$D = 0.4$	$D = 0.6$	$D = 0.8$
Rockfills from Shangzhai	0.5	50.2	39.4	30.1	20.1
	1	57.3	43.6	34.6	20.6
	2	80.2	63.7	54.2	38.2
	3	90.8	73.6	54.2	41.9
Redstone granular soil	0.05	–	37.7	12.9	8.2
	0.1		46.8	17.3	12.7
	0.2		50.2	16.1	12.1
	σ_3 (MPa)	$D = 0.25$	$D = 0.5$	$D = 0.75$	–
Rockfills from Dalian	0.4	128.5	100.8	69.5	–
	0.8	134.5	112.8	77.5	
	1.2	139.1	109.3	75.2	

4.1 Modification of the Young's modulus *E*

Figure 6a, b illustrates the relationship between the deviator stress $(\sigma_1 - \sigma_3)$ and the transient axial strain at different confining pressures for the rockfills from Shangzhai [36] and redstone granular soil [6], respectively. These two rockfills exhibit clear nonlinearities and stress-dependent stiffness. However, a constant Young's modulus is adopted in the classical Burgers model, which is clearly unsuitable for rockfills. Thus, Eq. (12) is introduced to calculate the tangent Young's modulus for rockfills, as adopted in the hyperbolic model proposed by Ducan and Chang [9]. The axial transient strain ε_1^0 is formulated in Eq. (13):

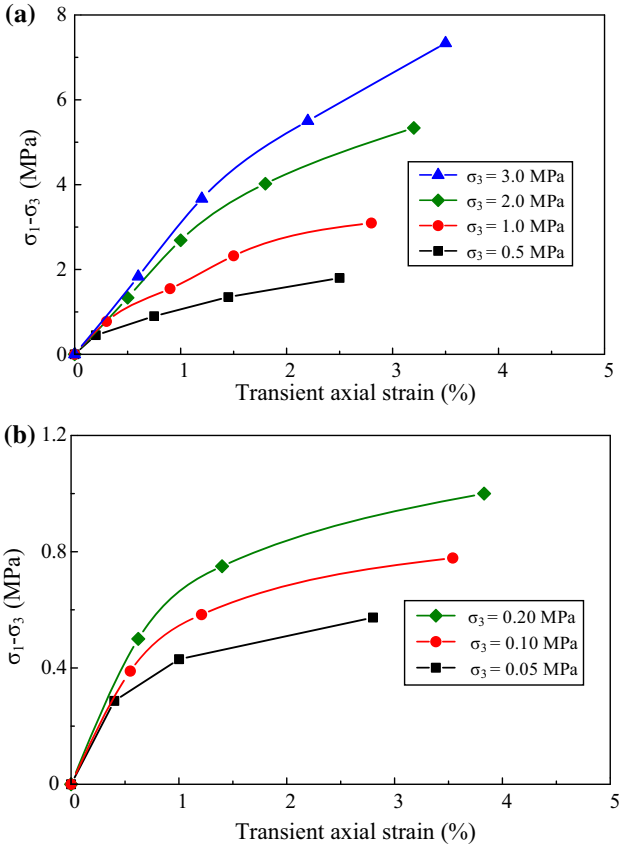

Fig. 6 $(\sigma_1 - \sigma_3)$ value versus the transient axial strain: **a** rockfills from Shangzhai [36] and **b** redstone granular soil [6]

$$E_t = (1 - R_f D)^2 K_1 p_a \left(\frac{\sigma_3}{p_a}\right)^{n_1} \tag{12}$$

$$\varepsilon_1^0 = \frac{1}{\left(\frac{1}{(\sigma_1 - \sigma_3)} - \frac{R_f}{(\sigma_1 - \sigma_3)_f}\right) K_1 p_a \left(\frac{\sigma_3}{p_a}\right)^{n_1}} \tag{13}$$

where p_a is the atmospheric pressure, K_1 and n_1 govern the values of the initial tangent modulus, $R_f = (\sigma_1 - \sigma_3)_f / (\sigma_1 - \sigma_3)_{ult}$, where $(\sigma_1 - \sigma_3)_f$ is the peak deviator stress and $(\sigma_1 - \sigma_3)_{ult}$ is the asymptotic value of $(\sigma_1 - \sigma_3)$ when the stress–strain curve approaches infinite strain. The three parameters (K_1, n_1, and R_f) can easily be obtained from a series of conventional triaxial tests under different σ_3 values.

4.2 Modification of the Newton viscosity coefficient η^N

Table 3 lists the η^N values of the three rockfills at different stress states, and Fig. 7 illustrates variations of η^N with the deviator stress levels and confining pressures. For the three materials, η^N is relatively constant at different deviator stress levels under the same σ_3 (Fig. 7a, c, e). However, η^N

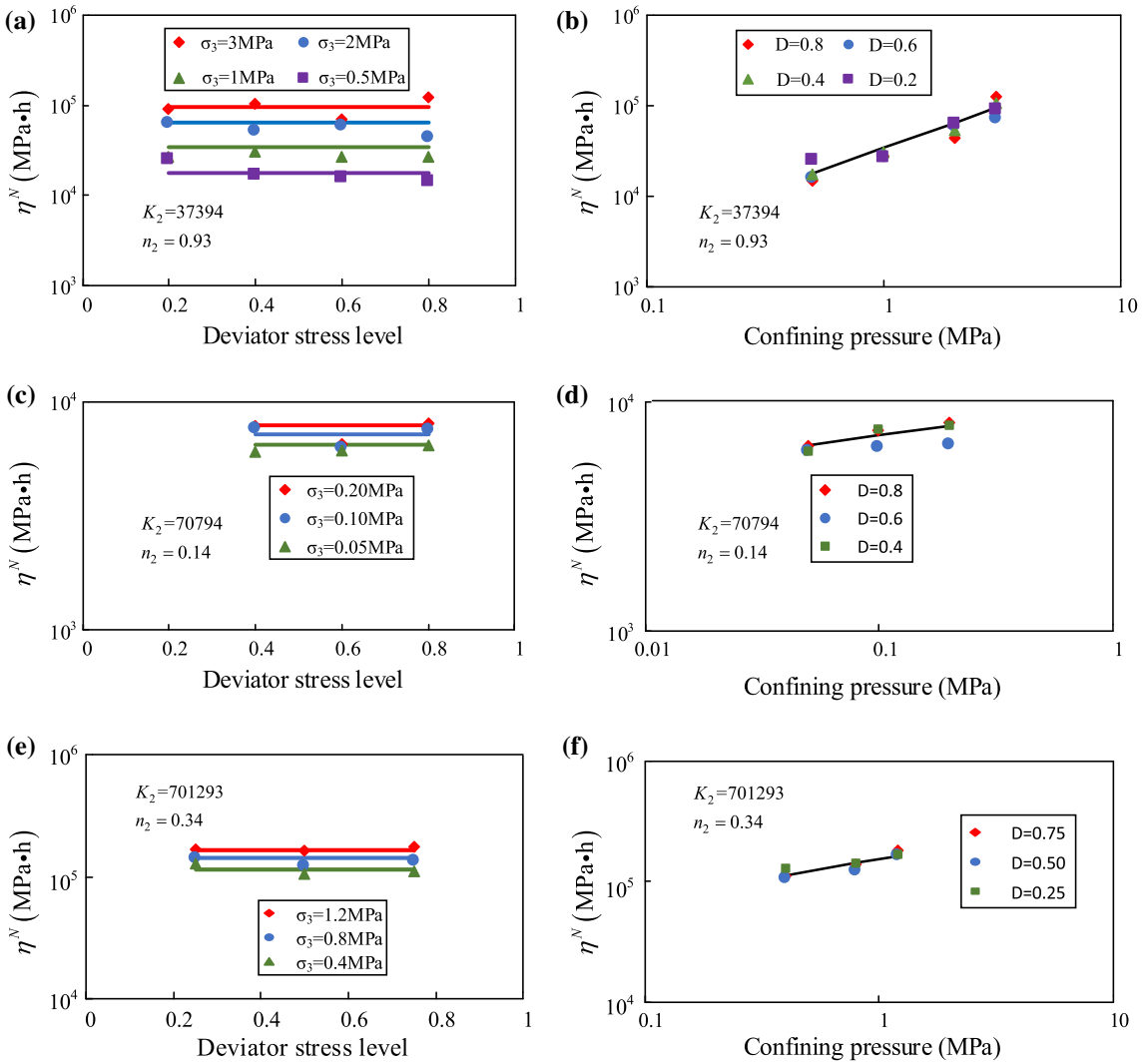

Fig. 7 Variation of η^N with deviator stress levels and confining pressures: **a**, **b** rockfills from Shangzhai [36]; **c**, **d** redstone granular soils [6]; **e**, **f** rockfills from Dalian [27]

increases almost linearly with the logarithm of σ_3 (Fig. 7b, d, f), which means that the confining pressure has significant influence on η^N. One possible reason for this influence may be that under a larger confining pressure, the particles are held together more tightly in the steady creep stage, which makes it more difficult to readjust their position and leads to a slower rate of the steady creep strain, i.e., a larger value of η^N.

Eq. (14) is proposed to approximately describe a linear relationship between $\log(\eta^N)$ and $\log(\sigma_3)$:

$$\frac{\eta^N(\sigma_3)}{p_a \cdot t_{ref}} = K_2 \left(\frac{\sigma_3}{p_a}\right)^{n_2} \tag{14}$$

where t_{ref} is set to one hour, and p_a is the atmospheric pressure. To eliminate dimensional effects, the η^N values are all normalized by the two indices (t_{ref} and p_a). K_2 and n_2 are two new parameters of the modified Newton viscosity coefficient, which can be back-determined by the least-square fitting method according to Eq. (14) and the calibrated values of η^N in Table 3. The solid lines in Fig. 7 are obtained by substituting the values of K_2, n_2, and the corresponding stress states into Eq. (14). Despite some scatter, the solid lines calculated by Eq. (14) are consistent with most of the η^N points. Hereby, the strain of the modified Newton unit in Eq. (1) is written as:

$$\varepsilon_i^{N,M} = \frac{q_i}{2K_2(p_a \cdot t_{ref})\left(\frac{\sigma_3}{p_a}\right)^{n_2}} t \tag{15}$$

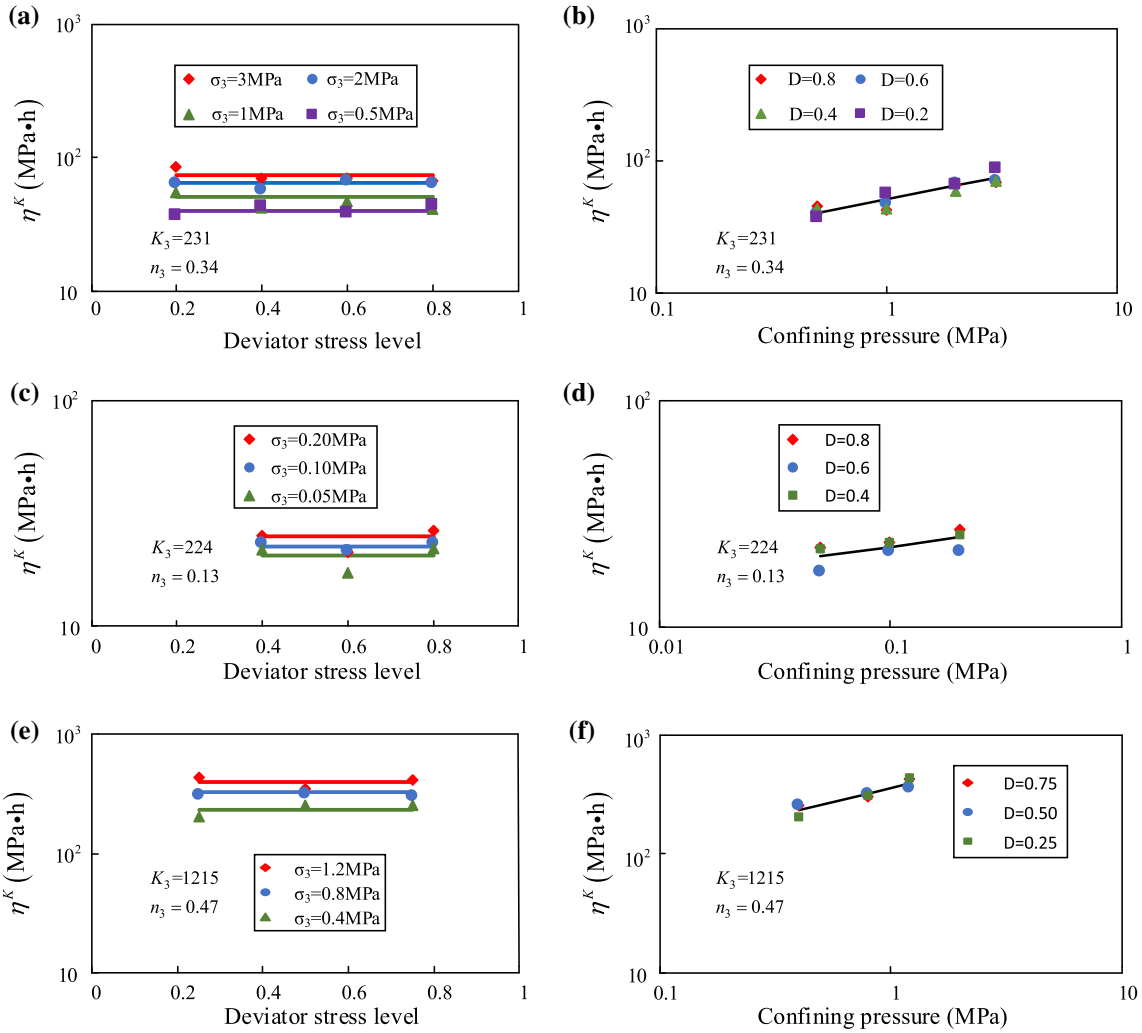

Fig. 8 Variation of η^K with deviator stress levels and confining pressures: **a**, **b** rockfills from Shangzhai [36]; **c**, **d** redstone granular soils [6]; **e**, **f** rockfills from Dalian [27]

4.3 Modification of the Kelvin viscosity coefficient η^K

The η^K values of the three rockfills are listed in Table 4 and are also plotted against the corresponding D and σ_3 values (Fig. 8). The deviator stress level D also appears to have insignificant influence on η^K if σ_3 remains unchanged. However, the value of η^K increases linearly with the logarithm of σ_3. Thus, η^K can also be regarded as dependent only on the confining pressure. Eq. (16) is proposed to describe the approximately linear relationship between $\log(\eta^K)$ and $\log(\sigma_3)$:

$$\frac{\eta^K(\sigma_3)}{p_a \cdot t_{ref}} = K_3 \left(\frac{\sigma_3}{p_a}\right)^{n_3} \tag{16}$$

where K_3 and n_3 are two new parameters of the modified Kelvin viscosity coefficient, which can be back-determined by the least-square fitting method according to Eq. (16) and the calibrated values of η^K in Table 4. As shown in Fig. 8, a fairly high consistency is observed between the points of η^K obtained from experimental results and the solid lines simulated by Eq. (16).

4.4 Modification of the Kelvin shear modulus G^K

Table 5 summarizes the G^K values of these three types of rockfills. The relevance of G^K and the corresponding stress states (i.e., the confining pressures and deviator stress levels) is demonstrated in Fig. 9. G^K tends to decrease with the deviator stress level (Fig. 9a, c, e). A possible mechanism is that more particle breakages or grain contact crushes occur when the sample is continuously subjected to a higher deviator stress level, which leads to the development of more time-dependent deformations. This phenomenon was also observed in previous studies [1, 16, 17, 23, 34]. An increasing trend of G^K is observed with the confining

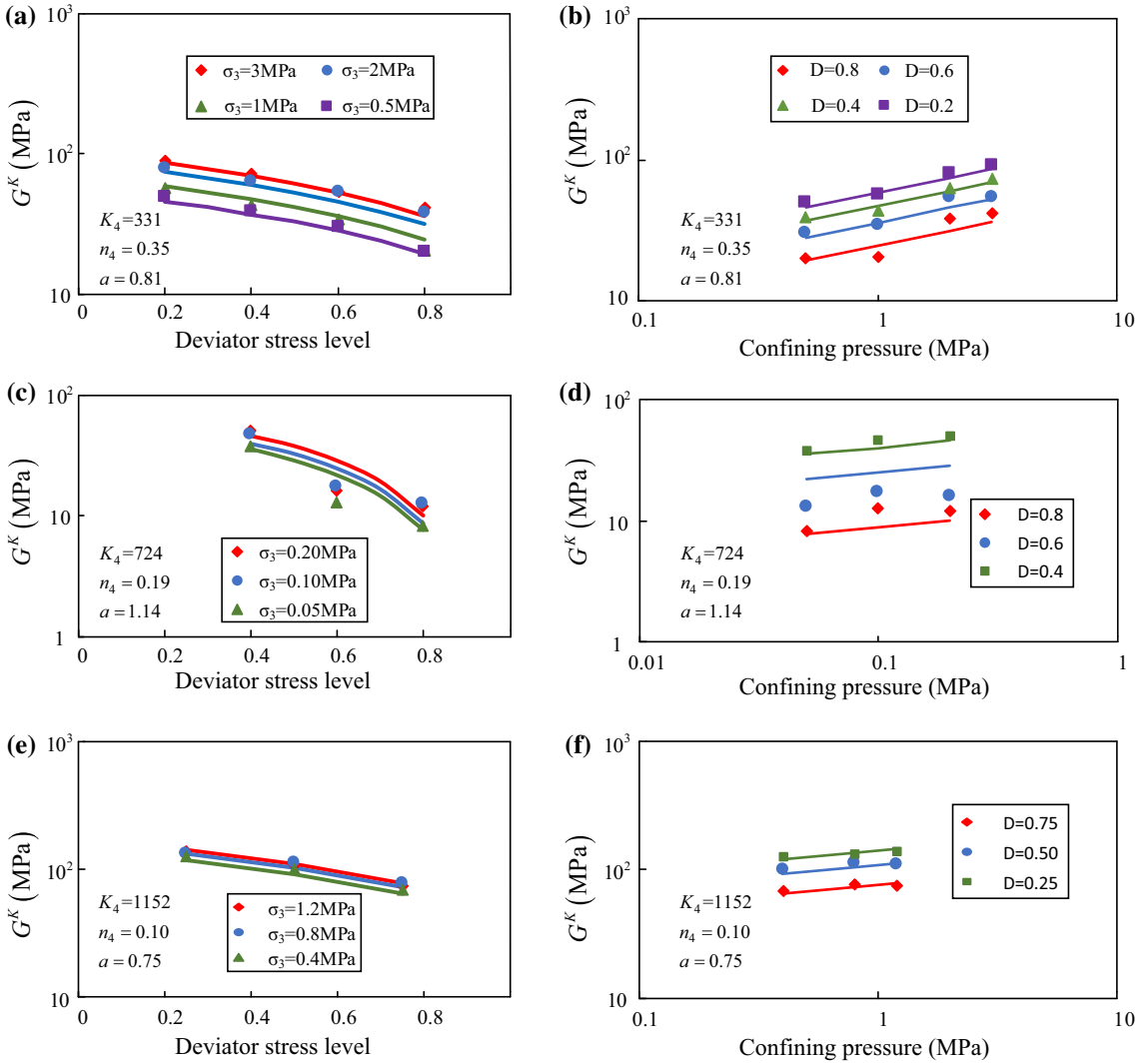

Fig. 9 Variations of G^K with deviator stress levels and confining pressures: **a**, **b** rockfills from Shangzhai [36]; **c**, **d** redstone granular soils [6]; **e**, **f** rockfills from Dalian [27]

pressure (Fig. 9b, d, f). Thus, Eq. (17) is proposed to consider the influence of both the deviator stress level and confining pressure:

$$\frac{G^K(\sigma_3, D)}{p_a} = K_4\left(\frac{\sigma_3}{p_a}\right)^{n_4}(1 - aD) \tag{17}$$

where the term $(1 - aD)$ is used to simulate the value of G^K decreasing with the deviator stress level, and a represents the decreasing rate. When $D = 0$, the modification of G^K has a form similar to that in Eqs. (14) and (16), which are used to simulate the effects of the confining pressure.

The three parameters (K_4, n_4, and a) can be obtained using the least squares fitting method according to Eq. (17) and the calibrated values of G^K in Table 5. The solid lines calculated by Eq. (17) are consistent with the points of G^K obtained from the experimental results (Fig. 9). Hereby, the strain of the modified Kelvin unit is

$$\varepsilon_i^{K,M} = \frac{q_i}{2K_4 p_a\left(\frac{\sigma_3}{p_a}\right)^{n_4}(1 - aD)\left[1 - \exp\left(-\frac{K_4}{K_3 t_{\text{ref}}}\left(\frac{\sigma_3}{p_a}\right)^{n_4 - n_3}(1 - aD)t\right)\right]} \tag{18}$$

In summary, the axial strain of the modified Burgers model ($\varepsilon_1^{B,M}$) is formulated as:

$$\varepsilon_1^{B,M} = \varepsilon_1^0 + \varepsilon_1^{N,M} + \varepsilon_1^{K,M} \tag{19}$$

where ε_1^0, $\varepsilon_1^{N,M}$, and $\varepsilon_1^{K,M}$ can be calculated by substituting the corresponding stress states and model parameters into Eqs. (13), (15), and (18), respectively.

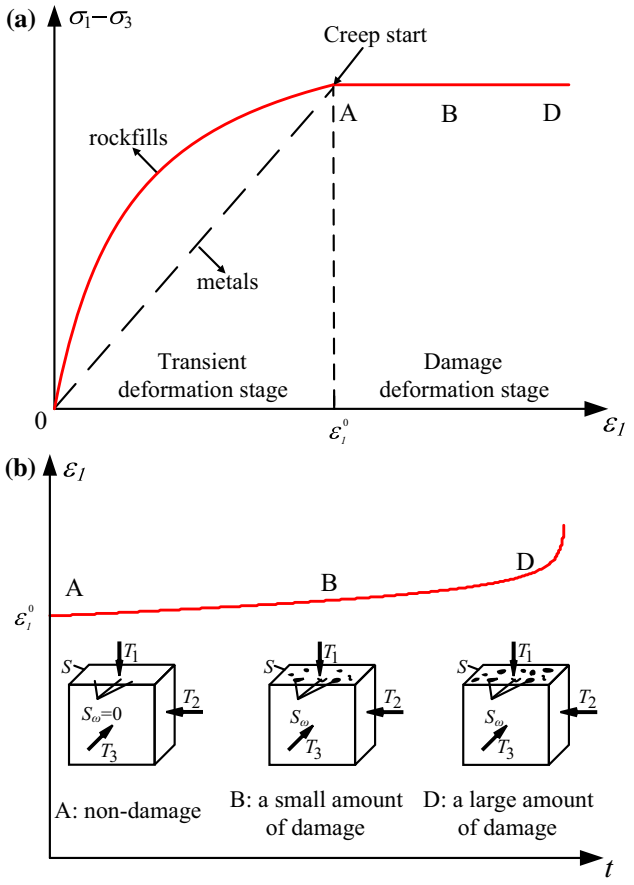

Fig. 10 Deformation process for a nonlinear elasto-damage unit

5 Nonlinear elasto-damage unit for rockfills considering accelerated creep behavior

The modified Burgers model proposed in Sect. 4 can reproduce the stress–stain and strain–time curves of rockfills in the attenuated and steady creep stages. However, the model cannot simulate the accelerated creep behavior of rockfills. To overcome this limitation, a nonlinear elasto-damage unit for rockfills is proposed. The stress–strain relation (solid line in Fig. 10a) of the nonlinear elasto-damage unit is classified into two stages: the transient deformation stage (OA) and the damage deformation stage (ABD). The deformation in the former stage (OA) was discussed in Sect. 4.1. This section aims to simulate the deformation in the latter stage (ABD). A critical threshold of the deviator stress level (D_{thr}) is first defined to determine whether the damage mechanism will be initiated after the beginning of creep (point A) by comparing D and D_{thr}: (1). If $D < D_{\text{thr}}$, the strain of the nonlinear elasto-damage unit remains unchanged: (2). If $D \geq D_{\text{thr}}$, the damage mechanism is initiated, and the strain of this unit accelerates over time, as demonstrated by the solid line in Fig. 10b. Because only limited experience has been gained for this parameter in previous research, laboratory tests are required to determine D_{thr}. D_{thr} is expected to be affected by a number of factors, including the mineral, gradation, and particle shape of rockfills. The following discussion is based on $D \geq D_{\text{thr}}$; i.e., the damage mechanism is initiated.

Kachanov [18] proposed a damage mechanism for metal. For the cubic damage unit in Fig. 10b, S is the overall section area of the unit and S_ω is the total area of the microcracks and cavities with different shapes. The damage variable ω is defined as $\omega = S_\omega/S$. Isotropic damage is assumed; i.e., the cracks and cavities are equally distributed in all directions. The strain of the unit in the damage deformation stage is calculated as:

$$\Delta\varepsilon_i^D = \varepsilon_i^{\text{ref}} \frac{\omega}{1-\omega} \tag{20}$$

$$\varepsilon_i^{\text{ref}} = \frac{(1+\upsilon)\sigma_i - \upsilon\sigma_{kk}}{E_{\text{t}}} \tag{21}$$

where $\varepsilon_i^{\text{ref}}$ is the referenced strain to calculate the creep strain in the accelerated creep stage, and E_{t} is the tangent elastic modulus. For metal, linear elasticity is assumed, and E_{t} is the slope of the dashed straight line in Fig. 10a. For rockfills, E_{t} is the tangent modulus of the hyperbolic curve at point A, which can be calculated from Eq. (12).

Different from metal, the influence of the deviator stress level should be considered for rockfills: A modified damage evolution law for rockfills is proposed as:

$$\frac{d\omega}{dt} = C\left(\frac{D}{1-\omega}\right)^V \tag{22}$$

where C and V are two parameters of the damage variables for rockfills, and D is the deviator stress level. The dimension of C is 1/hour. D and V are dimensionless. According to the initial condition, i.e., $\omega(0) = 0$, ω can be expressed as:

$$\omega = 1 - \left[1 - C(1+V)D^V t\right]^{\frac{1}{1+V}} \tag{23}$$

To determine C and V from creep test results, two intermediate variables (t_{ult} and γ) are introduced in Eqs. (24) and (25), respectively:

$$t_{\text{ult}} = \frac{1}{C(1+V)D^V} \tag{24}$$

$$\gamma = \frac{1}{1+V} \tag{25}$$

Thus, ω is rewritten as:

$$\omega = 1 - \left[1 - \frac{t}{t_{\text{ult}}}\right]^{\gamma} \tag{26}$$

Here, t_{ult} and γ are not new model parameters but are functions of the model parameters C and V. t_{ult} is called the "ultimate time," as sketched in Fig. 1. γ controls the rate at

which the damage variable increases with time. The dimension of t_{ult} is hour, and γ is dimensionless.

The results of the creep test on the redstone granular soil ($\sigma_3 = 50$ kPa and $D = 0.8$) performed by Chen and Zhang [6], in which the accelerated creep was observed, are used to illustrate the process to determine parameters. t_{ult} can be easily obtained from the vertical asymptote of the creep test strain. t_{ult} = 108 h is obtained based on the test results by Chen and Zhang [6]. γ is obtained through the following steps.

Step 1 Once the damage mechanism is initiated, the strain of the proposed model comprises the strain of the modified Burgers model ($\varepsilon_1^{B,M}$) and the strain in the damage deformation stage ($\Delta\varepsilon_1^D$). $\Delta\varepsilon_1^D$ can be separated from the measured axial strain in the test by removing the value of $\varepsilon_1^{B,M}$, as demonstrated in Fig. 11a

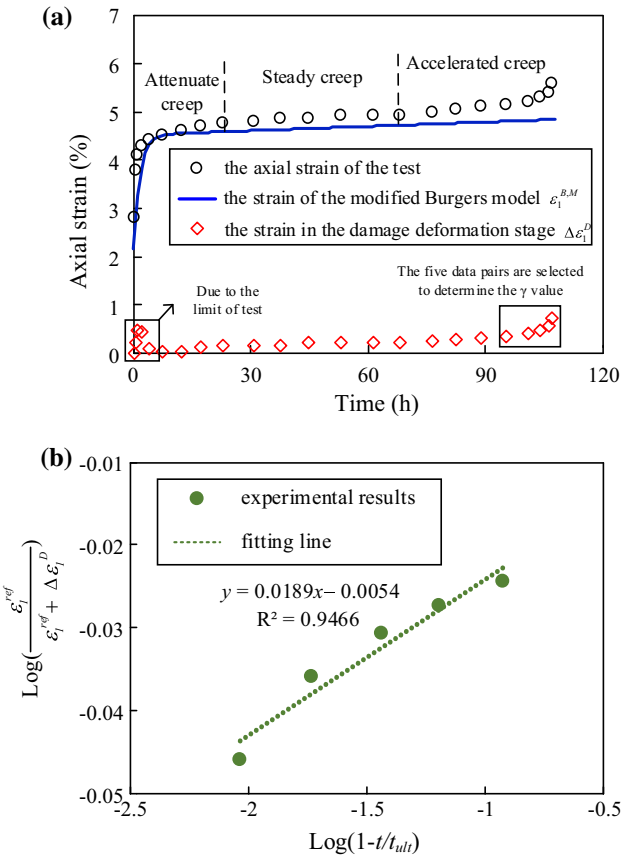

Fig. 11 Procedure to determine the parameters of the damage variable: **a** separating $\Delta\varepsilon_1^D$ from the measured axial strain; **b** the $\log\left(\frac{\varepsilon_1^{\mathrm{ref}}}{\varepsilon_1^{\mathrm{ref}}+\Delta\varepsilon_1^D}\right) - \log\left(1-\frac{t}{t_{\mathrm{ult}}}\right)$ curve and the fitting line for redstone granular soil ($D = 0.8$ and $\sigma_3 = 50$ kPa, [6])

Step 2 Equation (27) can be derived according to Eqs. (20) and (26):

$$\log\left(\frac{\varepsilon_i^{\mathrm{ref}}}{\varepsilon_i^{\mathrm{ref}}+\Delta\varepsilon_i^D}\right) = \gamma\log\left(1-\frac{t}{t_{\mathrm{ult}}}\right) \tag{27}$$

where $\varepsilon_i^{\mathrm{ref}}$ can be determined according to Eq. (21). By substituting the corresponding data of the last five red diamonds (Fig. 11a) into Eq. (27), $\log\left(\frac{\varepsilon_i^{\mathrm{ref}}}{\varepsilon_i^{\mathrm{ref}}+\Delta\varepsilon_i^D}\right)$ can be plotted against $\log\left(1-\frac{t}{t_{\mathrm{ult}}}\right)$, as shown in Fig. 11b. The slope of the fitting line equals γ.

By substituting the values of t_{ult} and γ in Eqs. (24) and (25), the corresponding parameters C and V can be determined, respectively. Analogously, the values of C and V of the redstone granular soil at $D = 0.8$ with the other two confining pressures ($\sigma_3 = 100, 200$ kPa) are obtained and listed in Table 6.

The values of $\log(V)$ and $\log(C)$ are further plotted against the corresponding $\log(\sigma_3/p_a)$ in Fig. 12a, b, respectively. The value of V is relatively constant at different confining pressures (Fig. 12a). However, a linearly decreasing relation between $\log(C)$ and $\log(\sigma_3/p_a)$ is observed (Fig. 12b). Thus, Eq. (28) is proposed to consider the influence of σ_3:

$$C = C_{\mathrm{ref}}\left(\frac{\sigma_3}{p_a}\right)^m \tag{28}$$

where C_{ref} and m are the intercept and slope of the fitting line in Fig. 12b. Therefore, t_{ult} is dependent on both the deviatoric stress level and the confining pressure.

In summary, the axial strain of the nonlinear elasto-damage unit proposed for rockfills is formulated as:

$$\varepsilon_1^D = \begin{cases} \varepsilon_1^0 & D < D_{\mathrm{thr}} \\ \varepsilon_1^0 + \varepsilon_1^{\mathrm{ref}}\dfrac{\omega}{1-\omega} & D \geq D_{\mathrm{thr}} \end{cases} \tag{29}$$

ε_1^0, $\varepsilon_1^{\mathrm{ref}}$, and ω can be calculated from Eqs. (13), (21), and (26), respectively.

6 Shear creep model for rockfills

By substituting Eqs. (15), (18), and (29) into Eq. (1), the axial strain of the shear creep model for rockfills is obtained as shown in Eq. (30):

Table 6 Parameters C and V of the redstone granular soil at different σ_3 values [6]

σ_3 (MPa)	0.05	0.1	0.2
C	17.74	15.57	7.47
V	49.1	51.6	46.6

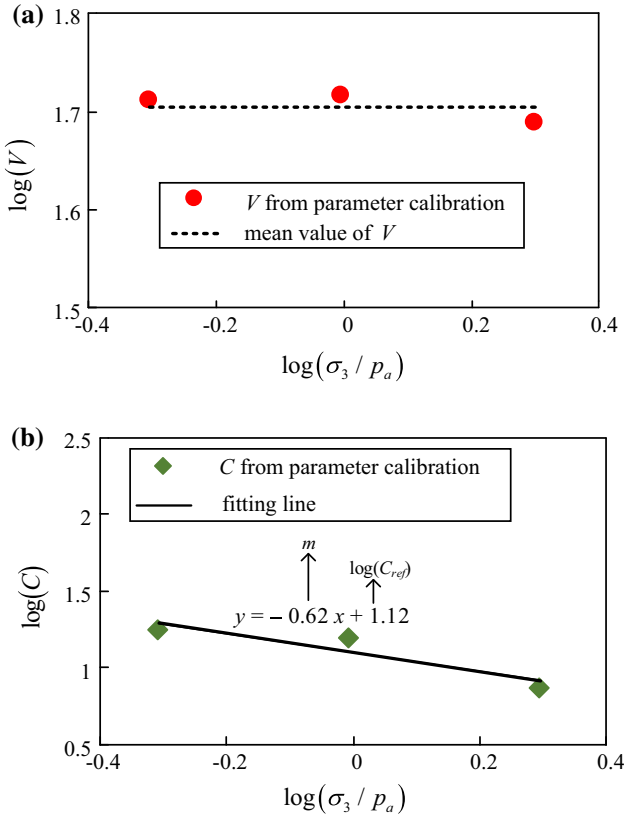

Fig. 12 Relation between the parameters of the damage variables and the confining pressures: **a** $\log(V)$ versus $\log(\sigma_3/p_a)$; **b** $\log(C)$ versus $\log(\sigma_3/p_a)$ (redstone granular soil, performed by [6])

$$\varepsilon_1 = \begin{cases} \varepsilon_1^0 + \dfrac{q_i}{2G^K(\sigma_3,D)}\left(1-\exp\left(-\dfrac{G^K(\sigma_3,D)}{\eta^K(\sigma_3)}t\right)\right) + \dfrac{q_i}{2\eta^N(\sigma_3)}t & D<D_{\text{thr}} \quad \text{(a)} \\ \varepsilon_1^0 + \dfrac{q_i}{2G^K(\sigma_3,D)}\left(1-\exp\left(-\dfrac{G^K(\sigma_3,D)}{\eta^K(\sigma_3)}t\right)\right) + \dfrac{q_i}{2\eta^N(\sigma_3)}t + \varepsilon_1^{\text{ref}}\dfrac{\omega}{1-\omega} & D\geq D_{\text{thr}} \quad \text{(b)} \end{cases} \tag{30}$$

1. If $t = 0$, $\varepsilon_1 = \varepsilon_1^0$, which represents the transient deformation (i.e., segment OA in Fig. 1). As introduced in Sect. 4.1, this model can capture the nonlinear stress–strain behaviors of rockfills (i.e., red solid line OA in Fig. 10a).
2. If $D < D_{\text{thr}}$, this model becomes the modified Burgers model, as proposed in Sect. 4, which can simulate the transient deformation, the deformation of the attenuated, and the steady creep stages. Eqs. (14), (16), and (17) are used to describe the variations of the parameters (η^N, η^K, and G^K) with the deviator stress levels and confining pressures.
3. If $D \geq D_{\text{thr}}$, the damage mechanism is initiated, and the corresponding strain and strain rate approach infinity when time approaches t_{ult}. Thus, this model has the capability to reproduce the accelerated creep behavior of rockfills.
4. The proposed model has a total of 14 parameters, as listed in Table 7. Ten of the parameters are used in the modified Burgers model, and the calibration methods are presented in Sect. 4. The other four parameters are used to describe the damage evolution of the damage variable ω, which can be determined by the method introduced in Sect. 5.

Table 7 Parameters of the shear creep models for rockfills

Nonlinear elasto-damage unit	E_t	K_1
		n_1
		R_f
	ω	C_{ref}
		m
		V
	D_{thr}	D_{thr}
Modified Newton unit	η^N	K_2
		n_2
Modified Kelvin unit	η^K	K_3
		n_3
	G^K	K_4
		n_4
		a

Table 8 Parameters of the proposed shear creep models for the three rockfills [6, 27, 36]

	Modified Newton unit		Modified Kelvin unit					Nonlinear elasto-damage unit						
	η^N		η^K		G^K			E_t			ω			Damage threshold
	K_2	n_2	K_3	n_3	K_4	n_4	a	K_1	n_1	R_f	C_{ref}	m	V	D_{thr}
Rockfills from Shangzhai	37,394	0.93	231	0.34	331	0.35	0.81	725	0.64	0.95	–		–	–
Rockfills from Dalian	701,293	0.34	1215	0.47	1152	0.10	0.75	–	–	–	–		–	–
Redstone granular soils	70,794	0.14	224	0.13	724	0.19	1.14	1230	0.10	0.95	13.18	– 0.62	51	0.8

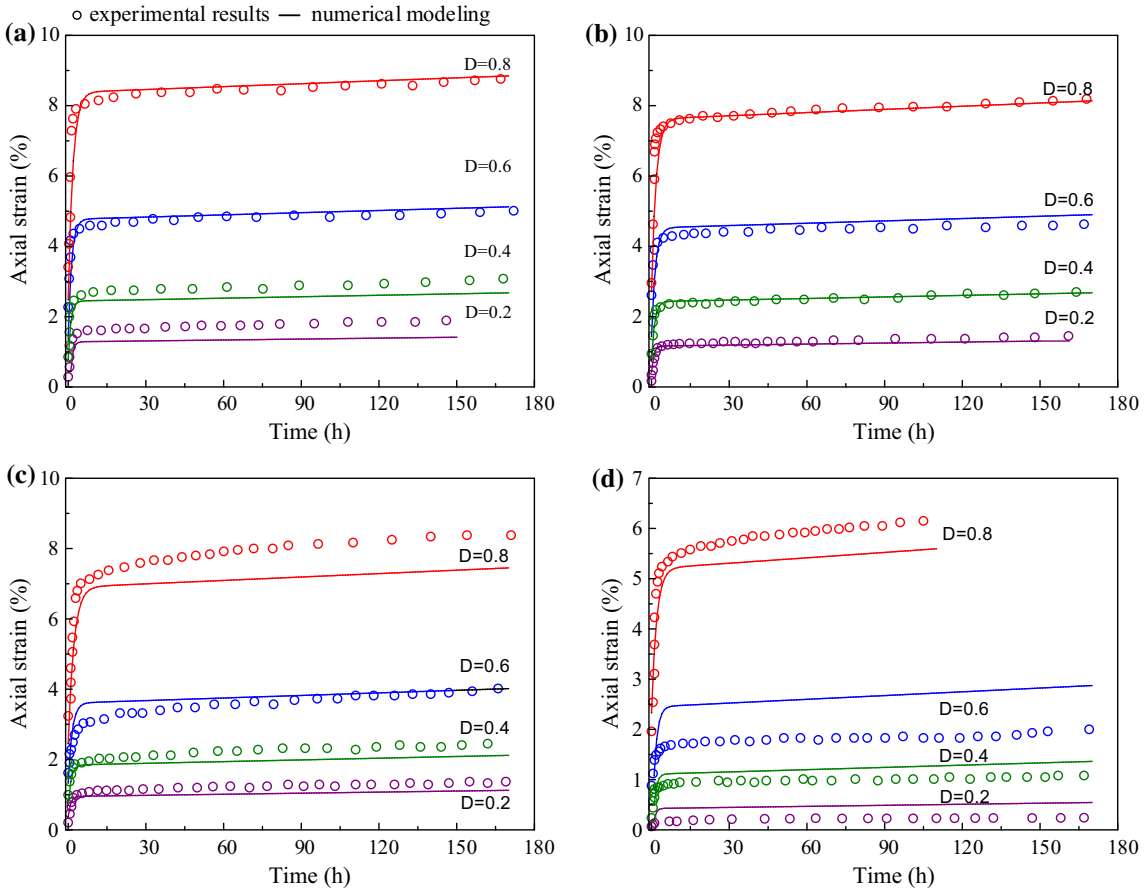

Fig. 13 Comparison between the simulation results and the creep test results on the rockfills from Shangzhai [36]: **a** $\sigma_3 = 3.0$ MPa, **b** $\sigma_3 = 2.0$ MPa, **c** $\sigma_3 = 1.0$ MPa, and **d** $\sigma_3 = 0.5$ MPa

7 Experimental test results and analysis

The results of the large-scale triaxial creep tests on three different rockfills [6, 27, 36] over a wide range of confining pressures and deviator stress levels are used to validate the proposed model, and their parameters are back-determined and listed in Table 8. The model-calculated lines are obtained by substituting the parameters and corresponding stress states into Eq. (30). As shown in Figs. 13, 14, and 15, the calculated results agree well with the experimental data. By using the same set of parameters for each type of rockfill, the proposed model not only can reflect the influence of D and σ_3 on the shear creep behavior but also can simulate all three creep stages of the rockfill, including the accelerated creep stage.

8 Conclusions

Rockfills have been used extensively for the construction of high-fill embankments and dams, which exhibit complex time-dependent behavior. This paper presents a rheological model to simulate the shear creep behaviors of rockfills based on the classic Burgers model, in which a nonlinear elasto-damage unit, a modified Newton unit, and a modified Kelvin unit are connected in series. By analyzing the results of large-scale triaxial creep tests on different rockfills, the influence of the stress state (i.e., the deviator stress level and confining pressure) on the shear creep behavior of rockfills is revealed. A method to modify the key model parameters (i.e., the transient elastic modulus, the Newton viscosity coefficient, the Kelvin shear modulus, and the Kelvin viscosity coefficient) is proposed to consider such influence and is incorporated into the proposed model. Furthermore, the accelerated creep behavior of rockfills is reproduced by a nonlinear elasto-damage unit, which is developed by modifying the damage mechanism proposed by Kachanov [18]. A critical threshold of the deviator stress level (D_{thr}) is defined to determine whether the accelerated creep stage will be initiated.

Despite its simplicity, the model can simulate the essential aspects of the shear creep behaviors of rockfills, and fairly high consistencies are found between the simulation results and the large-scale triaxial creep test results.

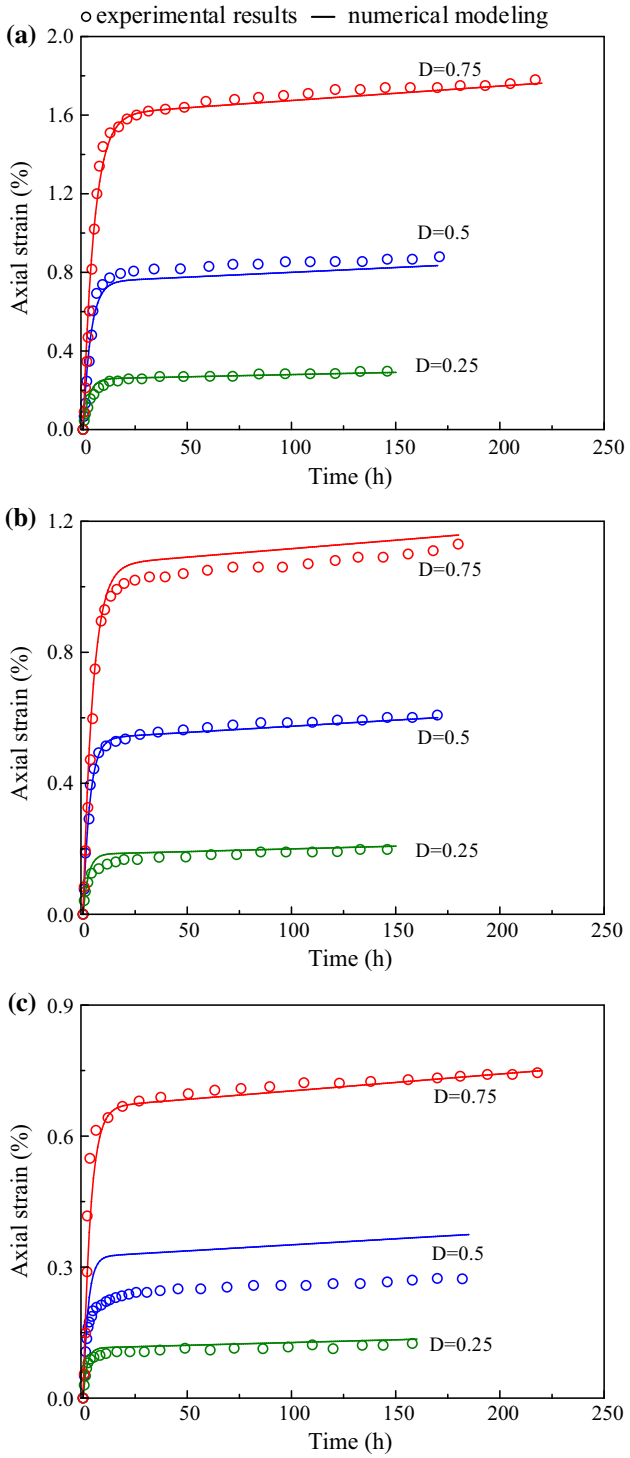

Fig. 14 Comparison between the simulation results and the creep test results on the rockfills from Dalian [27]: **a** $\sigma_3 = 1.2$ MPa, **b** $\sigma_3 = 0.8$ MPa, and **c** $\sigma_3 = 0.4$ MPa

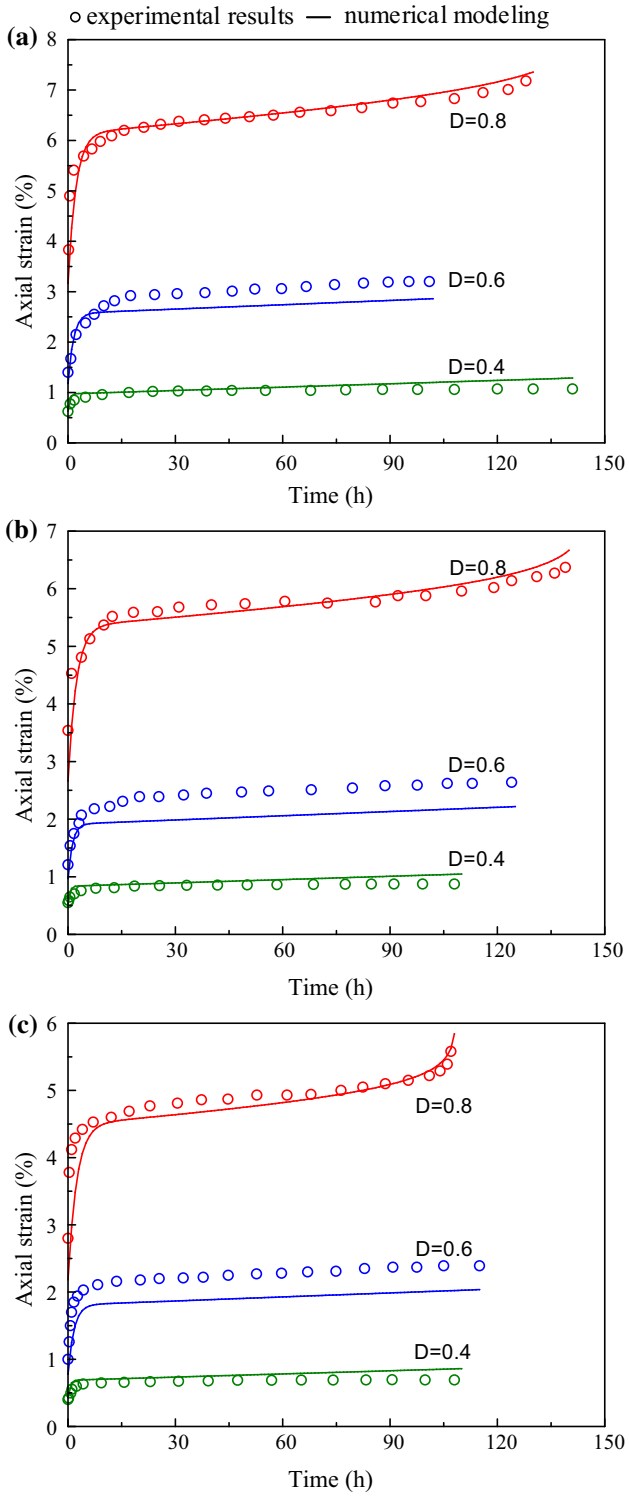

Fig. 15 Comparison between the simulation results and the creep test results on the redstone granular soils [6]: **a** $\sigma_3 = 0.2$ MPa, **b** $\sigma_3 = 0.1$ MPa, and **c** $\sigma_3 = 0.05$ MPa

However, this model is developed based on limited tests because only a few large-scale triaxial apparatuses exist that are capable of performing such long-term tests. Further laboratory studies are required to improve our understanding of the shear creep behavior of different rockfills and to improve this model.

Acknowledgements The authors are grateful for the research support received from the China 973 Program (2014CB047003) and the National Natural Science Foundation of China (41272280).

References

1. Alonso EE, Oldecop L, Pinyol NM (2009) Long term behaviour and size effects of coarse granular media. Mechanics of Natural Solids. Springer, Berlin, pp 255–281
2. Alonso EE, Romero EE, Ortega E (2016) Yielding of rockfill in relative humidity-controlled triaxial experiments. Acta Geotech 11:455–477
3. Anhdan L, Tatsuoka F, Koseki J (2006) Viscous effects on the stress-strain behavior of gravelly soil in drained triaxial compression. ASTM Geotech Test J 29(4):330–340
4. Canizal J, Castro J, Costa AD, Sagaseta C, Sola P (2015) High rockfills embankment for the extension of an airport main runway. In: Proceedings of the 15th Pan-American conference on soil mechanics and geotechnical engineering, Buenos Aires
5. Charles JA (2008) The engineering behaviour of fill materials, the use, misuse and disuse of case histories. Géotechnique 58(7):541–570
6. Chen X, Zhang J (2011) Large scale triaxial rheological apparatus development and granular soils rheological properties analysis. Appl Mech Mater 90–93(2011):79–89
7. Costa LM, Alonso EE (2009) Predicting the behavior of an earth and rockfills dam under construction. J Geotech Geoenviron Eng 135(7):851–862
8. Dounias GT, Anastasopoulos K, Kountouris A (2012) Long-term behaviour of embankment dams: seven Greek dams. Proc Inst Civ Eng Geotech Eng 165(3):157–177
9. Ducan J, Chang C (1970) Nonlinear analysis of stress and strain in soils. J Soil Mech Found Div 96:1629–1652
10. Enomoto T, Kawabe S, Tatsuoka F et al (2009) Effects of particle characteristics on the viscous properties of granular materials in shear. Soils Found 49(1):25–49
11. Enomoto T, Koseki J, Tatsuoka F et al (2016) Creep failure of natural gravelly soil and its simulation. Géotechnique 66(11):865–877
12. Findley WN, Lai JS, Onaran K et al (1976) Creep and relaxation of nonlinear viscoelastic materials with an introduction to linear viscoelasticity. North Holland, Amsterdam
13. Florkiewicz A, Kubzdela A (2013) Factor of safety in limit analysis of slopes. Geomech Eng 5(5):485–497
14. Griffiths DV, Marquez RM (2007) Three-dimensional slope stability analysis by elasto-plastic finite elements. Géotechnique 57(3):537–546
15. Jia Y, Chi S (2014) Back-analysis of soil parameters of the Malutang II concrete face rockfills dam using parallel mutation particle swarm optimization. Comput Geotech 65:87–96
16. Karimpour H, Lade PV (2010) Time effects relate to crushing in sand. J Geotech Geoenviron Eng 136(9):1209–1219
17. Karimpour H, Lade PV (2013) Creep behavior in Virginia Beach sand. Can Geotech J 50(11):1159–1178
18. Kachanov L (1958) Time of the rupture process under creep conditions. Izv Akad Nauk SSSR Otd Teck Nauk 8:26–31
19. Liang Z, Gong B, Tang C, Zhang Y, Ma T (2014) Displacement back analysis for a high slope of the Dagangshan hydroelectric power station based on BP neural network and particle swarm optimization. Sci World J 2014:741323-1–741323-11. https://doi.org/10.1155/2014/741323
20. Liingaard M, Augustesen A, Lade PV (2004) Characterization of models for time-dependent behavior of soils. Int J Geomech 4(3):157–177
21. Ma G, Zhou W, Ng TT, Cheng YG, Chang XL (2015) Microscopic modeling of the creep behavior of rockfills with a delayed particle breakage model. Acta Geotech 10:481–496
22. Mahinroosta R, Alizadeh A, Gatmiri B (2015) Simulation of collapse settlement of first filling in a high rockfills dam. Eng Geol 187:32–44
23. Michalowski RL, Nadukuru SS (2012) Static fatigue, time effects, and delayed increase in penetration resistance after dynamic compaction of sands. J Geotech Geoenviron Eng 138(5):564–574
24. Modares M, Quiroz JE (2015) Structural analysis framework for concrete-faced rockfills dams. Int J Geomech ASCE 16(1):04015024
25. Nagahara H, Fujiyama T, Ishiguro T, Ohta H (2004) FEM analysis of high airport embankment with horizontal drains. Geotext Geomembr 22(2):49–62
26. Seo MW, Ha IS, Kim YS, Olson SM (2009) Behavior of concrete-faced rockfills dams duringinitial impoundment. J Geotech Geoenviron Eng ASCE 135(8):1070–1081
27. Wang Z (2012) Experiment study on rheology of rockfills. Dissertation, Dalian University of Technology (in Chinese)
28. Won MS, Kim YS (2008) A case study on the post-construction deformation of concrete face rockfills dams. Can Geotech J 45(6):845–852
29. Wu Y, Yuan H, Zhang B, Zhang Z, Yu Y (2014) Displacement-based back-analysis of the model parameters of the Nuozhadu high earth-rockfill dam. Sci World J 2014:292450-1–292450-10. https://doi.org/10.1155/2014/292450
30. Xu M, Song E, Cao G (2009) Compressibility of broken rock-fine grain soil mixture. Geomech Eng 1(2):169–178
31. Xu M, Song E, Chen J (2012) A large triaxial investigation of the stress-path-dependent behavior of compacted rockfills. Acta Geotech 7(3):167–175
32. Xu M, Hong J, Song E (2017) DEM study on the effect of particle breakage on the macro- and micro-behavior of rockfill sheared along different stress paths. Comput Geotech 89:113–127
33. Xu M, Hong J, Song E (2018) DEM study on the macro- and micro-responses of granular materials subjected to creep and stress relaxation. Comput Geotech 102:111–124
34. Yamamuro JA, Abrantes AE, Lade PV (2011) Effect of strain rate on the stress-strain behavior of sand. J Geotech Geoenviron Eng 137(12):1169–1178
35. Zhang JM, Yang Z, Gao X, Zhang J (2015) Geotechnical aspects and seismic damage of the 156-m-high Zipingpu concrete-faced rockfills dam following the Ms 8.0 Wenchuan earthquake. Soil Dyn Earthq Eng 76:145–156
36. Zhang W (2013) Study on creep behavior and creep physical model of rockfills through triaxial creep test. China University of Geosciences (in Chinese)
37. Zhou W, Chang XL, Zhou CB, Liu XH (2010) Creep analysis of high concrete-faced rockfill dam. Int J Numer Methods Biomed Eng 26:1477–1492
38. Zhou MJ, Song E (2016) A random virtual crack DEM model for creep behavior of rockfill based on the subcritical crack propagation theory. Acta Geotech 11:827–847